THE JOURNAL OF BIOLOGICAL CHEMISTRY VOL. 290, NO. 13, pp. 8016–8027, March 27, 2015

Epidermal Growth Factor Receptor (EGFR) Signaling Requires a Specific Endoplasmic Reticulum Thioredoxin for the Post-translational Control of Receptor Presentation to the Cell Surface*[S]

Received for publication, November 1, 2014, and in revised form, February 9, 2015 Published, JBC Papers in Press, February 9, 2015, DOI 10.1074/jbc.M114.623207

Aiwen Dong, Dariusz Wodziak, and Anson W. Lowe[1]

From the Department of Medicine, Stanford University, Stanford, California 94305

Background: *AGR2* expression supports the transformed properties of many cancer cell lines.
Results: AGR2 protein functions as an endoplasmic reticulum thioredoxin that regulates EGFR presentation to the plasma membrane.
Conclusion: AGR2 controls EGFR-mediated signaling.
Significance: AGR2 represents a novel regulatory mechanism for signal transduction and a therapeutic target for EGFR-dependent cancers.

The epidermal growth factor receptor (EGFR) is a well characterized receptor-tyrosine kinase that functions in development and serves a vital role in many human cancers. Understanding EGFR regulatory mechanisms, and hence approaches for clinical intervention, has focused on ligand-receptor interactions and tyrosine kinase activity. Here, we show using the NCI-H460 lung and A431 epidermoid human cancer cell lines that EGFR binding to anterior gradient homolog 2 (*AGR2*) in the endoplasmic reticulum is required for receptor delivery to the plasma membrane and thus EGFR signaling. Reduced AGR2 protein levels or mutation of an essential cysteine in the active site result in decreased cell surface EGFR and a concomitant decrease in signaling as reflected by *AREG*, *EGR1*, and *FOS* expression. Similar to previously described *EGFR* nulls, an *AGR2* null also resulted in embryonic lethality. Consistent with its role in regulating EGFR-mediated signaling, *AGR2* expression is also enhanced in many human cancers and promotes the transformed phenotype. Furthermore, EGFR-mediated signaling in NCI-H460 cells, which are resistant to the tyrosine kinase inhibitor AG1478, is also disrupted with reduced *AGR2* expression. The results provide insights into why cancer prognosis or response to therapy often does not correlate with EGFR protein or RNA levels because they do not reflect delivery to the cell surface where signaling is initiated. AGR2, therefore, represents a novel post-translational regulator of EGFR-mediated signaling and a promising target for treating human cancers.

EGFR[2]-mediated signal transduction is initiated by soluble growth factors that bind the receptor at the cell surface (1–4). This binding promotes receptor dimerization and tyrosine phosphorylation of its cytoplasmic domain that initiates EGFR-mediated signaling and is followed by endocytosis and receptor degradation (5, 6). Since its discovery, EGFR has been closely linked with cancer pathogenesis (3). Most studies have focused on ligand-receptor binding, receptor kinase activation, and endocytosis as a means of regulating EGFR signaling (7). Another potential opportunity to regulate EGFR is through its presentation to the cell surface by the secretory pathway, a process for which little was known.

AGR2 is a 17-kDa protein that is expressed by many human cancers (8–15). *AGR2* expression promotes the transformed phenotype of adenocarcinoma cell lines by activating the Hippo signaling pathway co-activator YAP1, which in turn induces expression of an EGFR ligand, Amphiregulin (*AREG*) (16, 17). The specific mechanism by which AGR2 achieved its biological actions was unknown.

The AGR2 amino acid sequence is highly conserved across species from *Xenopus* to humans and contains a signal peptide and sequence homology to the thioredoxin superfamily (8, 18–20). We previously determined that AGR2's effects on signaling requires its residence in the endoplasmic reticulum (21). Seventeen members of the thioredoxin superfamily reside within the endoplasmic reticulum and function in protein folding by facilitating disulfide bond formation (20, 22). AGR2 features a CPHS amino acid sequence in its putative active site, which differs from the prototypic C*XX*C motif present in most thioredoxins. Only the first cysteine in the active site motif, however, is required for disulfide isomerase activity (23). A functional role for AGR2 as a thioredoxin had not been established, which led to a hypothesis that it serves such a role in the endoplasmic reticulum, and identification of its substrates would likely reveal how it directly affects signal transduction and cell transformation. In the present study we identify EGFR as an AGR2 substrate and show that this interaction is required for receptor presentation to the plasma membrane and signaling activity.

* This work was supported by the Stanford Division of Gastroenterology and Hepatology.
[S] This article contains supplemental Table 1.
[1] To whom correspondence should be addressed: Alway Bldg., Rm. M211, 300 Pasteur Dr., Stanford, CA 94305-5187. Tel.: 650-725-6764; Fax: 650-723-5488; E-mail: lowe@stanford.edu.
[2] The abbreviations used are: EGFR, epidermal growth factor receptor; AREG, amphiregulin; AGR2, anterior gradient homolog 2; ITGB1, integrin β1.

EXPERIMENTAL PROCEDURES

Reagents—The following antibodies were used for protein immunoblotting: anti-AGR2 (16), anti-EGFR (Cell Signaling, 2232), anti-phospho-EGFR (Abcam, ab40815), anti-EGR1 (Cell Signaling, 4153), anti-FOS (Cell Signaling, 2250), anti-ITGB1 (BD Biosciences, 610467), anti-GAPDH (Cell Signaling, 2118), anti-calnexin (Cell Signaling, 2433S), and anti-ACTB (Sigma, A2066). Antibodies used for immunoprecipitation include anti-AGR2 (Abnova, H00010551-M03), anti-EGFR that binds the mature protein (mAb 528, ATCC, HB-8509), and control mouse IgG2b (Santa Cruz Biotechnology, sc-2762). Other antibodies used for immunofluorescent staining include anti-ITGB (BioLegend, 303002) and anti-EGFR (Millipore, 06-847).

Cell Culture and Treatments—The lung adenocarcinoma cell line NCI-H460 and the epidermoid carcinoma cell line A431 (ATCC, Manassas, VA) were cultured according to protocols provided by the vendor. MCF-10A (ATCC) was cultured in DMEM/F-12 supplemented with 5% horse serum, 20 ng/ml EGF, 10 μg/ml insulin, 500 ng/ml hydrocortisone, and 100 ng/ml cholera toxin. After retroviral or lentiviral infection, cells were maintained in the presence of puromycin (2 μg/ml) (Sigma). For all *N*-ethylmaleimide experiments, cells were rinsed twice with ice-cold PBS and incubated with 20 mM *N*-ethylmaleimide in PBS for 10 min on ice. For the AG1478 (EGFR kinase inhibitor) experiments in the presence of serum, cells were plated 1 day before to reach 80% confluence when drug treatment was started. The culture media was replaced with fresh complete media containing 2 μM AG1478 for 1 h before the cells were collected for RNA extraction or protein immunoblotting. For Figs. 3, *D* and *E*, and 4, *C* and *D*, cells were serum-starved 16 h and treated with 2 μM AG1478 for 40 min followed by a 20-min stimulation with 100 ng/ml EGF in the absence of serum. For EGF stimulation (Fig. 3, *F* and *G*, Fig. 4, *E* and *F*), the cells were serum-starved for 16 h and followed by a 20-min treatment with EGF (100 ng/ml) in the absence of serum before the cells were collected with TRIzol (Invitrogen, 15596-026) for RNA extraction. For the induction of endoplasmic reticulum stress as a positive control, NCI-H460 cells were treated with 2 μg/ml tunicamycin or mock-treated with DMSO. Total RNA was collected 4 h later for quantitative PCR analysis of endoplasmic reticulum stress markers.

Virus Production and Infection—The LinX packaging cell line (Thermo Scientific, Open Biosystems, LNX1500) was used for the generation of retroviruses, and the 293T packaging cell line (Thermo Scientific Open Biosystems, HCL4517) was used for lentiviral amplification. The shAGR2 construct was generated as previously described (17). shAGR2 was transduced into NCI-H460 cells using retrovirus and A431 cells with lentivirus. shEGFR was expressed from pGIPZ lentiviral vector from Open Biosystems (Thermo Scientific Open Biosystems, Clone ID V3LHS_361962) and was used to infect both H460 and A431 cells. Viruses were collected 48 and 72 h after transfection, filtered, and used for infecting cells in the presence of 8 μg/ml Polybrene. Retroviral empty vector shRNA control (Thermo Scientific Open Biosystems, EAV4679) or GIPZ non-silencing lentiviral shRNA control (Thermo Scientific Open Biosystems, RHS4346) served as controls for shAGR2 and shEGFR, respectively. Optimal targeting sequences identified for human *AGR2* were 5′-CTGATTAGGTTATGGTTTAA-3′ and 5′-TGCTGAAGACTGAATTGTA-3′ and for human *EGFR* was 5′-TGGTGTGTGCAGATCGCAA-3′. Knockdown efficiency was assessed by quantitative real-time PCR and protein immunoblotting.

Statistical Analysis—The significance of differences between treatment groups was measured with the unpaired two tailed Student's *t* test (GraphPad Software, San Diego, CA). p values of <0.05 were considered statistically significant.

Co-immunoprecipitation of Mixed Disulfides—*N*-Ethylmaleimide (20 mM)-treated cells were lysed in cell lysis buffer (20 mM Tris HCl, pH 8.0, 137 mM NaCl, 2 mM EDTA, 1% Nonidet P-40, and 10% glycerol with protease inhibitor mixture) for 1 h. 5 mg of whole cell extracts were incubated with 2 μg of anti-AGR2 antibody (Abnova, H00010551-M03) or control mouse IgG2b (Santa Cruz Biotechnology, sc-2762) for 1 h. The protein complexes were precipitated by the addition of protein G-agarose beads (Millipore, 16-266) with incubation for 16 h at 4 °C. The beads were washed with cell lysis buffer 4 times and boiled for 5 min in sample buffer with or without 0.1 M dithiothreitol. The eluents were analyzed with protein immunoblotting. Mass spectrometry was used to identify AGR2 binding proteins. Briefly, 30 mg of whole cell extracts were incubated with 10 μg of anti-AGR2 antibody. The beads were washed 4 times, and after the last wash bound proteins were eluted with 0.1 M glycine HCl, pH 2.7, into tubes containing 0.1 M Tris HCl, pH 9.0.

Real-time PCR Analysis—3 μg of RNA sample was reverse-transcribed with GoScript Reverse Transcriptase System (Promega, A5003) to generate cDNA, which was subjected to SYBR Green-based real-time PCR analysis. Primers used were: AGR2 forward (5′-ATGAGTGCCCACACAGTCAA-3′) and reverse (5′-GGACATACTGGCCATCAGGA-3′); AREG forward (5′-GTGGTGCTGTCGCTCTTGATA-3′) and reverse (5′-ACTCACAGGGGAAATCTCACT-3′); EGFR forward (5′-CCCACTCATGCTCTACAACCC-3′) and reverse (5′-TCGCACTTCTTACACTTGCGG-3′); EGR1 forward (5′-GTACAGTGTCTGTGCCATGGATTTC-3′) and reverse (5′-GAGGATCACCATTGGTTTGCTTG-3′; FOS forward (5′-CACTCCAAGCGGAGACAGAC-3′) and reverse (5′-AGGTCATCAGGGATCTTGCAG-3′); β-actin forward (5′-GCACAGAGCCTCGCCTT-3′) and reverse (5′-GTTGTCGACGACGAGCG-3′); HSPA5 forward (5′-CACAGTGGTGCCTACCAAGA-3′) and reverse (5′-TGTCTTTTGTCAGGGGTCTTT-3′); HERPUD1 forward (5′-AGTGTGGGCCACCTCAAG-3′) and reverse (5′-TGGTGATCCAACAACAGCTT-3′).

Immunofluorescence Staining—Cells were fixed with 4% paraformaldehyde at room temperature for 15 min, rinsed twice with PBS, quenched with 0.15 M glycine, 5% BSA in PBS for 5 min 2 times, washed with PBS 3 times, and blocked with 5% BSA in PBS for 30 min. When noted, staining was performed using permeabilized cells, which consisted of adding 0.25% Triton X-100, 1% BSA, PBS for 15 min before blocking with bovine serum albumin. The slides were then incubated with anti-EGFR (mAb 528, 1:200), anti-EGFR (Millipore, 1:200), anti-AGR2 (1:100), or anti-ITGB1 (1:200) diluted in 1% BSA, PBS at 4 °C overnight. After overnight incubation, unbound primary antibodies were removed by washing the slides 5 times with PBS.

Appropriate Alexa Fluor® 594- or 488-conjugated secondary antibody (Invitrogen, 1:500) was added to the slide for 1 h at room temperature in the dark. The slides were then washed 5 times with PBS and mounted using VECTASHIELD antifade reagent (Vector Laboratories, H1200) with DAPI nuclear stain. The slide was imaged using a Nikon TS-1 confocal microscope (Nikon C1 system) with a 60× objective lens.

Subcellular Fractionation—MCF-10A cells transfected with either AGR2 or vector were plated in 150-mm dishes. Isolation of plasma membranes and microsomes was performed as previously described under the following conditions (24). After two washes with ice-cold PBS, cells were carefully harvested into 3 ml of homogenization buffer (225 mM mannitol, 75 mM sucrose, 0.1 mM EGTA, 5 mM Tris-HCl, pH 7.4, 1× protease inhibitor mixture) with a rubber policeman and transferred to a prechilled 5 ml Kontes Potter-Elvehjem homogenizer. Homogenization was performed for 5 strokes with steady and consistent pressure. The homogenate was transferred into a cooled polypropylene tube (Falcon 2059) and centrifuged at 600 × *g* for 3 min (HB-4 rotor, Sorvall). The supernatant (S1) was reserved and centrifuged again at 600 × *g* for 3 min. The resultant supernatant (S2) was then centrifuged for 20 min at 20,000 × *g* and 4 °C (70Ti rotor, Beckman), which produced a pellet (P3) enriched in plasma membranes. The supernatant was centrifuged at 100,000 × *g* for 1 h (Ti70, Beckman), which produced a pellet (P4) enriched in microsomal membranes. The pellet was resuspended in 100 μl of 300 mM sucrose, 10 mM Hepes, pH 7.4.

Site-directed Mutagenesis—AGR2-C81A was produced with the QuikChange II XL mutagenesis kit (Stratagene) using human AGR2 cDNA and expressed from the pcDNA3.1 vector (Life Technologies) (16). References to the AGR2 amino acid sequence are derived from NCBI accession code NP_006399.

Flow Cytometry—EGFR expression at the plasma membrane was determined by plating cells in 60-mm dishes. Twenty-four hours later the culture media was replaced with serum-free media for 1 h. The cells were washed with PBS, detached with Cell Dissociation Buffer (Invitrogen, 13151-014), and collected into tubes containing complete media on ice. Cells were washed 4 times with Cell Staining Buffer (BioLegend, 420201) and blocked with 5% BSA in PBS for 15 min at room temperature. After four washes with Cell Staining Buffer, cells were incubated with allophycocyanin-labeled anti-EGFR (BioLegend, 352905) or isotype control (BioLegend, 400121) for 45 min at 4 °C in the dark. Flow cytometry data were acquired using the Scanford (FACScan, Cytek) and analyzed with FlowJo v10 software (TreeStar).

Isolation of Cell Surface Biotinylated Proteins—Cell surface proteins were labeled covalently using a membrane-impermeant biotinylation reagent EZ-Link Sulfo-NHS-Biotin (Pierce, 21217). The following steps were carried out at 4 °C to prevent any trafficking; cells were washed 3 times with PBS^{2+} (PBS with 0.1 mM $CaCl_2$, 1 mM $MgCl_2$) followed by a 30-min incubation with 1 mg/ml Sulfo-NHS-Biotin in PBS^{2+}, washed twice with PBS^{2+}, and quenched twice with 50 mM glycine in PBS^{2+} for 5 min. After four washes with PBS^{2+}, the cells were lysed while on the plate (1% Triton X-100, 150 mM NaCl, 10% glycerol, 50 mM HEPES pH 7.5, 0.1% SDS, 0.5% sodium deoxycholate, 1 mM Na_3VO_4, 2 mM EDTA, and a protease inhibitor mixture (Sigma, P8340)) followed by centrifugation for 10 min at 16,000 × *g*. The protein concentration of the cleared lysate was determined using the bicinchoninic acid assay (Pierce, 23228 and 23224). 200 μg of protein samples were transferred to new tubes, and the volume was brought up to 400 μl with lysis buffer before streptavidin beads (GE Healthcare, 17511301) were added and agitated at 4 °C for 3 h. The beads were collected by centrifugation (7000 × *g*) and washed 4 times with lysis buffer at 4 °C followed by an incubation at 95 °C in Laemmli sample buffer. Equivalent volumes were analyzed with protein immunoblotting followed by densitometry of the resultant bands with a flatbed scanner and ImageJ (imagej.nih.gov). For Fig. 2*G*, NCI-H460-shAGR2 cells were plated in six 60-mm dishes and transfected with vector control, wild-type AGR2, or the AGR2 C81A mutant with Lipofectamine 2000 (Invitrogen). Forty-eight hours post-transfection, cell surface proteins were labeled with biotin or left unlabeled as described above.

Generation of AGR2 Null Mice—Embryonic stem cells were obtained from the University of California, Davis KOMP repository ($Agr2^{tm1(KOMP)Vlcg}$, cataloge number 17054). The *AGR2* null construct featured the replacement of *AGR2* exons 2–8 with a *lacZ* reporter. The cells were injected into blastocysts by the Stanford University Transgenic Research Facility and propagated in C57BL/6 mice. Germ line transmission was established and bred using standard procedures.

RESULTS

AGR2 Forms a Mixed Disulfide with EGFR—Based on the hypothesis that AGR2 acts as a thioredoxin, AGR2 should form a mixed-disulfide reaction intermediate with its substrate(s). NCI-H460 lung adenocarcinoma cells were used to identify potential substrates because *AGR2* expression is necessary for the cells' transformed properties (16, 17). *N*-Ethylmaleimide, which alkylates free sulfhydryl moieties, was administered to the NCI-H460 cells to promote the persistence of mixed-disulfides and enhance detection of AGR2 substrates (25). AGR2 antibodies were then employed to isolate mixed-disulfide complexes from homogenates of *N*-ethylmaleimide-treated or untreated NCI-H460 cells by immune precipitation followed by protein immunoblotting with AGR2 antisera produced in a different species. If the samples were left unreduced to retain the mixed-disulfide complexes, major bands ~170 kDa were detected that disappeared or decreased in intensity if the samples were initially reduced with dithiothreitol, therefore, supporting their identity as AGR2 mixed disulfides (Fig. 1*A*). EGFR was suspected as a potential AGR2 substrate because of its known mass and the previously characterized effects of AGR2 on EGFR signaling via *AREG* expression (16). Protein immunoblotting with EGFR antisera of the same AGR2 immune-precipitated mixed disulfide samples revealed bands identical to those previously visualized with the AGR2 antisera, therefore, identifying EGFR as a potential AGR2 substrate (Fig. 1*B*). The AGR2-EGFR mixed disulfide was also detected with protein immunoblotting of *N*-ethylmaleimide-treated NCI-H460 whole cell lysates by protein immunoblotting (Fig. 1*C*).

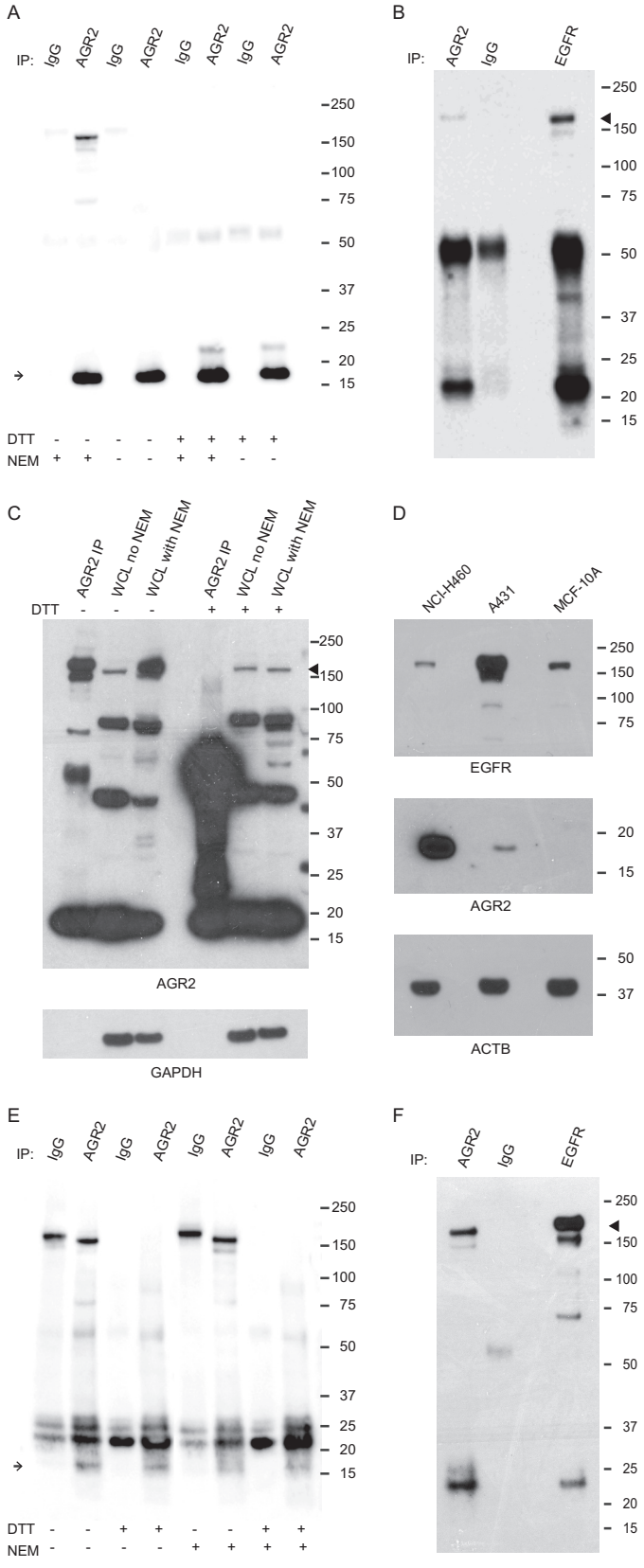

FIGURE 1. AGR2 forms mixed-disulfides in NCI-H460 (*A* and *B*) and A431 (*E* and *F*) cells. *A* and *E*, immune precipitates (*IP*) from *N*-ethylmaleimide (*NEM*)-treated or untreated cells collected with control IgG or mouse anti-AGR2 antibodies and detected with protein immunoblotting using rabbit anti-AGR2 antibodies. Before SDS-PAGE, the samples were unreduced (−) or reduced (+) with 0.1 M dithiothreitol (*DTT*). The band at ~180 kDa in the unreduced IgG lane most likely represents nonspecific binding to intact immunoglobulin. The expected AGR2 band is seen at ~17 kDa (*arrow*). *B* and *F*, immune precipitation of cells with anti-AGR2, nonspecific IgG, or anti-EGFR antibodies followed by protein immunoblotting of dithiothreitol-reduced samples with anti-EGFR antibodies. Immune precipitation with the anti-EGFR antibody served as a positive control for the EGFR band (*arrowhead*). *C*, protein immunoblots of whole cell lysates (*WCL*) probed with anti-AGR2 antibody to detect AGR2 mixed disulfides in the absence of contaminating antibodies. Immune precipitates from *N*-ethylmaleimide-treated NCI-H460 cells with anti-AGR2 antibody were run alongside as controls. The samples were unreduced (−) or reduced (+) with 0.1 M DTT before SDS-PAGE. GAPDH served as a loading control. *D*, protein immunoblots for EGFR, AGR2, and β-actin (ACTB) in NCI-H460, A431, and MCF-10A whole cell lysates. 10 μg was loaded in each lane.

The experiments were repeated with A431 cells, a cell line derived from an epidermoid carcinoma that is often used as a model system because of its high *EGFR* expression (26). Previous studies have shown that AREG expression is also strongly induced by EGFR signaling (27, 28). Whether A431 cells are also dependent on AGR2 for EGFR signaling and AREG expression was evaluated. Protein immunoblotting established that A431 cells also express AGR2 (Fig. 1*D*). Transduction of the A431 cells with shAGR2 led to an 15.8-fold decrease in AGR2 RNA along with a concomitant 10.2-fold decrease in *AREG* expression and established that it is influenced by AGR2 expression in A431 cells. *N*-Ethylmaleimide treatment of A431 cells also preserved AGR2 mixed disulfides with EGFR that were disrupted with a reducing agent (Fig. 1, *E* and *F*). AGR2 immune precipitates from A431 cells were also analyzed by mass spectrometry, which identified EGFR as the top candidate with respect to the number of total unique peptides and the total spectrum count (supplemental Table S1). No other ErbB family members were detected in the mass spectrometry analysis. Together, the results support a physical interaction between AGR2 and EGFR.

AGR2 Expression Regulates EGFR Expression at the Plasma Membrane—The most common role ascribed to endoplasmic reticulum-based thioredoxins is the folding or assembly of proteins through the formation of disulfide bonds (29). Secretory proteins that have attained the appropriate confirmation are then allowed to progress to the Golgi apparatus and the remainder of the secretory pathway. Proteins that are unable to achieve the appropriate conformation are exported from the endoplasmic reticulum and destroyed in the proteasome. An evaluation was, therefore, initiated to determine whether *AGR2* interactions with EGFR influence receptor delivery to the plasma membrane. Our previous studies showed that transduction with shAGR2 is able to reduce AGR2 RNA and protein in NCI-H460 cells by 11- and 9-fold (16). Two different shAGR2 sequences were used to decrease AGR2 expression, which resulted in similar results on *AGR2* expression.

Immunocytochemistry was performed using non-permeabilized NCI-H460 and A431 cells that were labeled with a monoclonal antibody (mAb528) that binds the mature EGFR ectodomain at the cell surface (30, 31). Compared with vector controls, a striking decrease in EGFR cell surface staining in both NCI-H460 and A431 cells was observed after *AGR2* expression was reduced with shAGR2 (Fig. 2*A*). As a control, no changes in cell surface expression of integrin, β1 (*ITGB1*) were observed in either cell line after AGR2 knockdown (Fig. 2*B*). Immunocytochemistry was also performed on detergent-per-

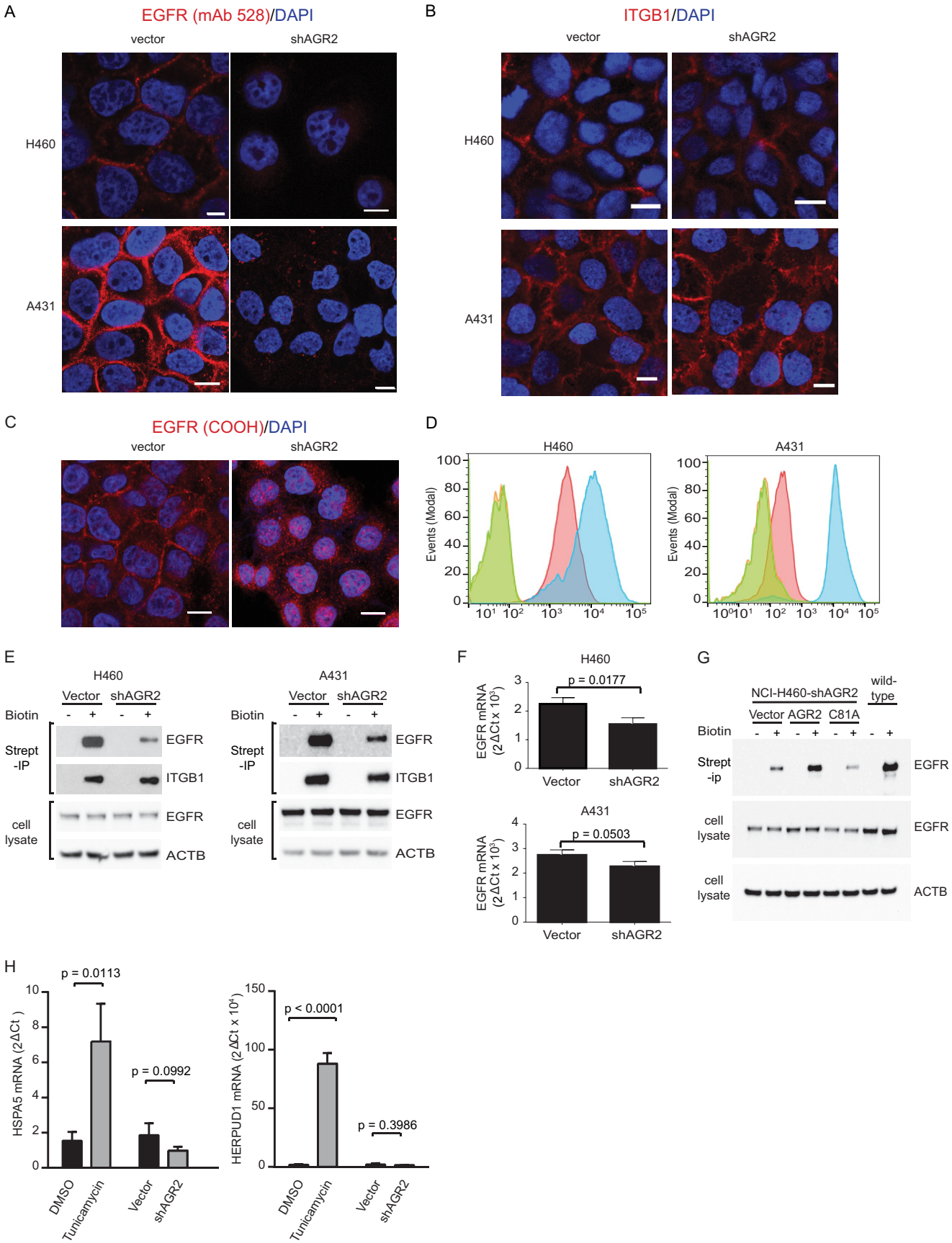
A
EGFR (mAb 528)/DAPI
vector
shAGR2
H460
A431
B
ITGB1/DAPI
vector
shAGR2
H460
A431
C
EGFR (COOH)/DAPI
vector
shAGR2
D
H460
A431
Events (Modal)
E
H460
A431
Vector
shAGR2
Biotin
Strept -IP
cell lysate
EGFR
ITGB1
ACTB
F
H460
p = 0.0177
EGFR mRNA (2ΔCt x 10^5)
Vector
shAGR2
A431
p = 0.0503
G
NCI-H460-shAGR2
Vector
AGR2
C81A
wild-type
Biotin
Strept -ip
cell lysate
EGFR
ACTB
H
p = 0.0113
p = 0.0992
HSPA5 mRNA (2ΔCt)
p < 0.0001
p = 0.3986
HERPUD1 mRNA (2ΔCt x 10^4)
DMSO
Tunicamycin
Vector
shAGR2

meabilized NCI-H460 cells with an anti-cytoplasmic domain EGFR antibody, which also revealed a decrease in cell surface EGFR with shAGR2 reduction of AGR2 expression. The anti-cytoplasmic antibody was also able to detect significant amounts of intracellular EGFR (Fig. 2*C*).

Further validation of decreased cell surface *EGFR* expression with shAGR2 was obtained with flow cytometry. Flow cytometry with anti-EGFR antibodies determined that the mean cell surface EGFR expression decreased by 5- and 58-fold compared with vector controls in NCI-H460 and A431 cells, respectively, after *AGR2* expression was reduced with shRNA (Fig. 2*D*). A third approach biotinylated all cell surface proteins, which was followed by their isolation with streptavidin beads. The relative amount of biotinylated cell surface EGFR was determined by protein immunoblotting. A 4- and 10-fold decrease in plasma membrane EGFR after transduction with shAGR2 was observed in NCI-H460 and A431 cells, respectively, compared with vector controls (Fig. 2*E*). ITGB1 was used as a plasma membrane control and displayed a 0- and 1.8-fold decrease in NCI-H460 and A431 cells, respectively. Quantitative RT-PCR for EGFR transcripts revealed no significant difference between wild-type and shAGR2-treated cells (Fig. 2*F*). Likewise, an evaluation for changes in total EGFR protein secondary to shAGR2 also revealed no significant changes when compared with β-actin (Fig. 2, *E* and *G*). After transduction with shAGR2, EGFR is present within the cell and not on the cell surface (Fig. 2, *C* and *G*). Additional control experiments assessed for the presence of endoplasmic reticulum stress in the context of transduction with shAGR2. Analysis of HSPA5 and HERPUD1 revealed no signs of endoplasmic reticulum stress (Fig. 2*H*), which is consistent with our published work and that of others (32–34). The data, therefore, demonstrate that cell surface EGFR was determined by its cellular distribution rather than the total amount of receptor in the cell.

As a control for potential off target effects of shAGR2, rescue experiments were performed with NCI-H460-shAGR2 cells that express low AGR2 levels. Transduction of NCI-H460-shAGR2 cells with wild-type AGR2 cDNA that is insensitive to shAGR2 resulted in increased AGR2 expression and plasma membrane EGFR (Fig. 2*G*). Further supporting AGR2's function as a thioredoxin, plasma membrane EGFR levels were not enhanced when the cells were transduced with AGR2 cDNA harboring a C81A active site mutant that is predicted to destroy enzymatic activity. AGR2, therefore, acts as a thioredoxin and interacts with EGFR in the endoplasmic reticulum, which is necessary for receptor delivery to the cell surface. Considering recent studies have demonstrated that most EGFR-mediated signaling occurs at the plasma membrane (5, 6), AGR2 is well positioned to regulate EGFR-mediated signaling.

AGR2 Expression Is Necessary for EGFR-mediated Signaling—Experiments were performed to determine whether EGFR signaling is dependent on *AGR2* expression. EGFR activation results in receptor phosphorylation and an increase in *EGR1* and *FOS* expression, which were used as functional readouts (1, 27, 28, 35). Reduction of *EGFR* expression with shEGFR in A431 cells propagated in media containing serum resulted in a decline of EGFR phosphorylation and EGR1 and FOS protein and RNA (Fig. 3, *A*–*C*). Similar reductions in EGFR phosphorylation and EGR1 and FOS RNA and protein were also observed when the A431 cells were incubated with the EGFR-specific tyrosine kinase inhibitor AG1478 (36). When *AGR2* expression was likewise reduced in A431 cells with shAGR2, reductions in EGFR phosphorylation and EGR1 and FOS protein and RNA were observed. The reduction in *AGR2* expression with shAGR2 did not result in a significant change in total EGFR protein, which is consistent with an effect on subcellular redistribution (Fig. 3*A*). EGFR-mediated signaling is, therefore, dependent on *AGR2* expression.

Instead of serum, signaling was also induced with the addition of EGF (100 ng/ml) to the media of serum-starved cells, which resulted in marked induction of *EGR1* and *FOS* expression. The EGFR-specific tyrosine kinase inhibitor, AG1478, significantly inhibited the EGF-induced expression in the A431 cells (Fig. 3, *D* and *E*). Reduction of AGR2 expression with shAGR2 dramatically reduced EGF-stimulated *EGR1* and *FOS* expression (Fig. 3, *F* and *G*).

Decrease AGR2 Expression Effectively Reduces EGFR Signaling in Cells Resistant to a Tyrosine Kinase Inhibitor—Reducing EGFR transport to the plasma membrane is a potentially more effective approach for disrupting EGFR signaling than receptor inhibition at the cell surface. Consistent with previous studies (37), the EGFR-specific tyrosine kinase inhibitor, AG1478, was ineffective at concentrations up to 50 μM in NCI-H460 cells in inhibiting *EGR1* or *FOS* expression in the presence of serum (Fig. 4, *A* and *B*). Reducing AGR2 expression with shRNA, however, readily reduced *EGR1* and *FOS* expression in NCI-H460 cells.

FIGURE 2. **AGR2 determines EGFR cell surface expression.** Immunofluorescence with anti-EGFR mAb 528 (*A*) or anti-ITGB1 antibodies (*B*) to label non-permeabilized NCI-H460 and A431 cells transduced with a vector control or shAGR2. The nuclei were labeled with DAPI stain (*blue*). Identical exposure settings were used to obtain all the images. *Scale bar* = 10 μm. *C*, immunocytochemistry with anti-cytoplasmic domain EGFR (COOH) antibodies of detergent-permeabilized NCI-H460 cells transduced with a vector control or shAGR2. *Scale bar* = 10 μm. *D*, flow cytometry with allophycocyanin-conjugated anti-EGFR antibodies labeling NCI-H460 or A431 cells transduced with a vector control (*blue*) or shAGR2 (*red*). Allophycocyanin-conjugated isotype control antibodies were included to label NCI-H460 or A431 cells transduced with a lentiviral vector control (*green*) or shAGR2 (*orange*). The signal intensity is plotted on the *abscissa* and the number of events on the *ordinate*. *E*, detection of plasma membrane EGFR with cell surface biotinylation. Vector control or shAGR2-transduced NCI-H460 and A431 cells were cell surface-labeled with biotin (+) followed by affinity purification with streptavidin beads. Seven percent of the purified proteins were assessed for EGFR and integrin B1 with protein immunoblotting. The whole cell lysates represent 20% (NCI-H460) and 5% (A431) of the starting material used for the affinity purification and serve as a positive control. *IP*, immunoprecipitate. *F*, quantitative RT-PCR of EGFR mRNA in NCI-H460 and A431 cells with and without shAGR2. Values are normalized to β-actin. *G*, rescue experiments demonstrating shAGR2 specificity were performed using cell surface biotinylation for plasma membrane EGFR. AGR2 rescue of NCI-H460-shAGR2 cells by transducing with a vector control, wild-type AGR2, or AGR2-C81A mutant is shown. Cell surface proteins were purified from 200 μg of cell lysate and assayed for EGFR as described for *E*. Wild-type NCI-H460 cells served as a positive control and were processed in a similar manner. Protein immunoblots for EGFR in the cell lysates were included as a positive control. *ACTB*, β-actin. *H*, reduced AGR2 expression does not trigger ER stress. Quantitative real-time-PCR analysis of HSPA5 and HERPUD1 RNA in NCI-H460 cells treated with tunicamycin (2 μg/ml) or shAGR2 is shown.

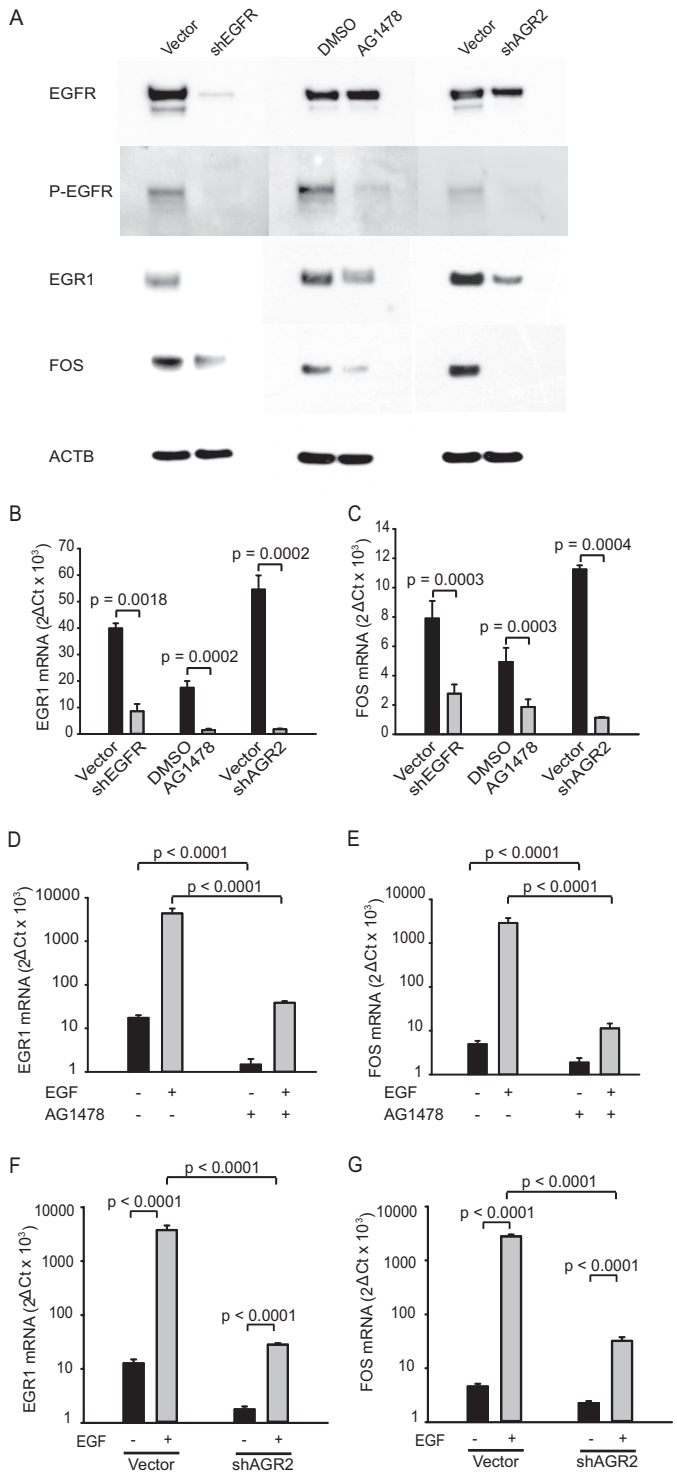

FIGURE 3. **EGFR-mediated signaling is dependent on AGR2 expression.** *A*, protein immunoblots for EGFR, phosphorylated EGFR (*EGFR-P*), EGR1, FOS, and β-actin (*ACTB*) of whole cell lysates derived from A431 cells propagated in serum-containing media after transduction with a vector control, shEGFR, shAGR2, or treated with the EGFR tyrosine kinase inhibitor AG1478 (2 μM). *B* and *C*, quantitative real-time-PCR analysis of *EGR1* (*B*) and *FOS* (*C*) RNA in A431 cells similarly treated with shEGFR, AG1478 (2 μM), and shAGR2. *D* and *E*, quantitative real-time-PCR analysis of *EGR1* (*D*) and *FOS* (*E*) RNA in A431 cells similarly treated with EGF (100 ng/ml) with and without AG1478 (2 μM). *F* and *G*, quantitative real-time-PCR analysis of *EGR1* (*F*) and *FOS* (*G*) RNA in A431 cells transduced with vector control or shAGR2. Cells were first serum-starved for 16 h followed by a 20-min treatment with 100 ng/ml EGF. Data are presented relative to β-actin and shown as the mean ± S.D. of triplicates. *p* value, two-tailed unpaired *t* tests.

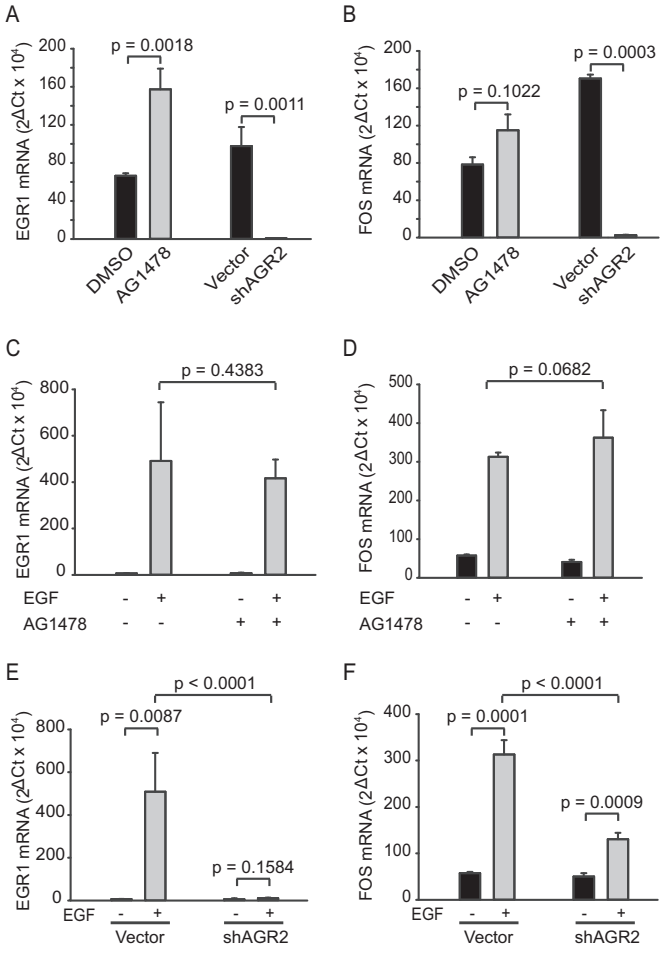

FIGURE 4. **Reduced AGR2 expression decreases EGFR signaling in tyrosine kinase inhibitor-resistant cells.** *A* and *B*, quantitative real-time-PCR analysis of *EGR1* (*A*) and *FOS* (*B*) RNA in NCI-H460 cells treated with AG1478 (2 μM) and shAGR2. *C* and *D*, effect of AG1478 on *EGR1* (*C*) and *FOS* (*D*) expression in serum-free conditions with and without EGF (100 ng/ml). *E* and *F*, response of *EGR1* (*E*) and *FOS* (*F*) expression to EGF stimulation in NCI-H460 cells transduced with a vector control or shAGR2. Cells were first serum-starved for 16 h followed by a 20-min treatment with 100 ng/ml EGF. Data are presented relative to β-actin and shown as the mean ± S.D. of triplicates. *p* value, two-tailed unpaired *t* tests.

Similar results were obtained when EGF was employed in lieu of serum to stimulate EGFR-mediated signaling. EGF addition to the media resulted in a 77- and 5-fold increase of *EGR1* and *FOS* mRNA expression that was not affected by the tyrosine kinase inhibitor, AG1478 (Fig. 4, *C* and *D*). In contrast, shAGR2 significantly reduced the effects of EGF stimulation (Fig. 4, *E* and *F*). Manipulating AGR2, therefore, exhibited greater efficacy in inhibiting EGFR signaling than the tyrosine kinase inhibitor.

Recombinant AGR2 Expression Alone Is Sufficient to Stimulate EGFR Plasma Membrane Delivery—The experiments presented thus far showed that reducing *AGR2* expression in transformed cells decreases cell signaling secondary to EGFR's absence from the cell surface. The converse experiment was also performed in which AGR2 was expressed in two non-transformed cell lines MCF-10A and CHO-K1 that do not express AGR2 (38, 39). MCF-10A cells are a non-transformed epithelial cell line derived from human fibrocystic breast tissue. Immunocytochemistry revealed that the MCF-10A cells are

heterogeneous and that very few cells express AGR2 (0.5%, n = 598 cells; Figs. 1*D* and 5*D*).[3]

EGFR protein expression was evaluated with an anti-cytoplasmic domain antibody that detected strong EGFR staining within detergent-permeabilized MCF-10A cells. After transduction with AGR2 cDNA, the same antibody detected EGFR at the plasma membrane (Fig. 5*A*). Immunocytochemistry of detergent-permeabilized MCF-10A cells was also performed with monoclonal antibody 528, which detects mature EGFR that is endoglycosidase H-resistant, and revealed an increase in EGFR cell surface expression after transduction with AGR2 cDNA (Fig. 5*A*, *bottom*). In contrast, monoclonal antibody 528 detected much less intracellular EGFR compared with the anti-cytoplasmic domain antibody in vector control MCF-10A cells, suggesting that much of the protein possesses immature glycosylation.

The results with monoclonal antibody 528 are consistent with *AGR2* expression facilitating EGFR delivery to the Golgi apparatus where complex glycosylation occurs (40). Protein immunoblotting of MCF-10A cell lysate that was resolved with a low percentage SDS-PAGE gel showed that the EGFR mass increased with *AGR2* expression, which is consistent with maturation in glycosylation that occurs with progression in the secretory pathway (Fig. 5*B*). In addition, several bands between 50 and 100 kDa that are believed to represent EGFR degradation were detected mainly in cells transduced with the vector control.

Subcellular fractionation was also employed to show the transfer of EGFR protein from the endoplasmic reticulum to the plasma membrane after *AGR2* expression. EGFR protein in the plasma membrane fraction increased 4.9-fold after AGR2 transduction of MCF-10A cells (Fig. 5*C*).

AGR2 mixed disulfides were also purified from the MCF-10A in a manner similar to that described for the NCI-H460 and A431 cells. A ~170-kDa AGR2 reactive band was visualized in non-reduced conditions only for AGR2-transduced MCF-10A cells, which disappeared after reduction with dithiothreitol (Fig. 5*D*). Protein immunoblotting confirmed that the band was EGFR (Fig. 5*E*). The data again demonstrated that EGFR is the major AGR2 mixed disulfide (Fig. 5*D*).

Cell surface biotinylation was used to biochemically demonstrate that significant plasma membrane delivery of EGFR was achieved only after MCF-10A cells were transduced with AGR2 (Fig. 5*F*). Transduction with AGR2 harboring the C81A active site mutant did not promote EGFR delivery to the plasma membrane. Cell surface ITGB1 did not change with AGR2 expression. Significant amounts of EGFR protein were detected whether or not AGR2 was present in the MCF-10A cells (Fig. 5*F*).

AGR2-induced EGFR delivery to the plasma membrane was also reconstituted in CHO-K1 cells, which are negative for both EGFR and AGR2 expression. Transient transfection of CHO-K1 cells with an EGFR-GFP construct alone resulted in an intracellular distribution. Co-transfection with EGFR-GFP and AGR2 cDNA resulted in EGFR cell surface expression (Fig. 5*G*).

[3] A. Dong, D. Wodziak, and A. W. Lowe, personal observation.

AGR2 Null Mice Are Not Viable—A homozygous *EGFR* null mutation most often results in embryonic lethality, although strain-dependent differences may result in a small percentage (5–16%) that live as long as 3 weeks (41, 42). If AGR2 is necessary for EGFR-mediated signal transduction, then the *AGR2* null mutant should exhibit features similar to that of the *EGFR* null. Three previously published studies by different laboratories, including our own, generated conditional *AGR2* null mice that resulted in viable mice with histologic changes in the stomach and intestines that preferentially affected secretory cell lineages (32, 33, 43). One potential source for the different outcomes of the *AGR2* null from that of the *EGFR* null mice was that all three prior studies utilized floxed *AGR2* exons whose excision were dependent on the constitutive expression of Cre recombinase. Therefore, a definitive non-conditional null mouse was generated with germ line deletions of *AGR2* exons 2–8. Heterozygotes alone compared with heterozygote with wild-type matings resulted in average litter sizes of 4.4 and 6.2, respectively. Heterozygote matings resulted in only 2 (3.8%) viable offspring that were homozygous *AGR2* null mice (Table 1). One homozygote died at 3 weeks. The remaining homozygote that was sacrificed at 6 weeks was 27% smaller by weight than its heterozygous littermate and manifested many of the gastrointestinal changes previously observed with the conditional *AGR2* null (32). Overall, the outcomes of the *AGR2* null mirrored that of the published *EGFR* null mice.

DISCUSSION

This study presents a novel mechanism for controlling EGFR-mediated signal transduction. We demonstrate that an endoplasmic reticulum-based thioredoxin is able to dictate signaling activity by determining whether EGFR is delivered to the plasma membrane from the secretory pathway. Consistent with the endoplasmic reticulum's established role, proteins must attain the appropriate conformation before they can proceed to the Golgi apparatus and the plasma membrane. Protein folding and assembly in the endoplasmic reticulum is largely facilitated by the heat shock and thioredoxin protein families (29). AGR2's homology to other thioredoxins, its formation of mixed disulfides with EGFR, and loss of AGR2 function after mutating the putative active site cysteine are consistent with a role in establishing the appropriate disulfide bonds in EGFR. Appropriately assembled EGFR is then able to exit the endoplasmic reticulum to the plasma membrane where signaling is transduced (44). AGR2 enables EGFR transport to the cell surface and thus impacts cell signaling without affecting receptor RNA or protein levels.

The discovery of EGFR as a substrate is consistent with our previous observations that characterized AGR2's effects on signal transduction (16). Induced *AREG* expression by AGR2 is compatible with the activation of EGFR-mediated signaling. Recent gene expression studies revealed that *AREG* is one of the most highly induced genes by EGFR signaling and thus may serve as a marker of signaling activity (27, 28). With respect to the previously reported impact of AGR2 expression on YAP1 activity, recent studies of *Drosophila* and human cells demonstrated that EGF signaling induces YAP1 activation by inhibiting its phosphorylation through the Ajuba proteins (45). It is

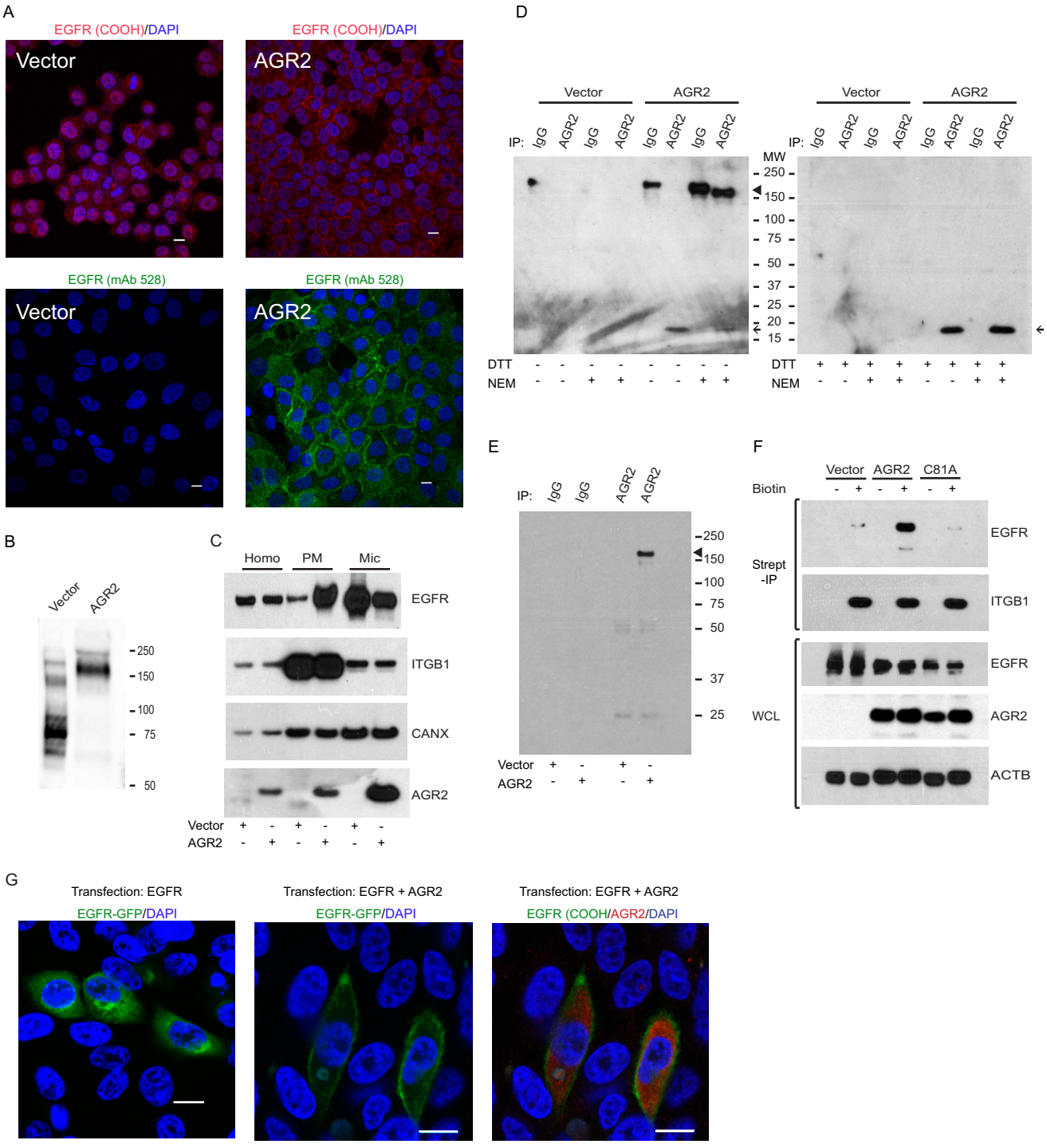

FIGURE 5. **Recombinant AGR2 expression in MCF-10A and CHO-K1 cells results in EGFR plasma membrane delivery.** *A*, immunocytochemistry of permeabilized MCF-10A cells with anti-cytoplasmic (*red*, *top panels*) or mAb 528 (*green*, *bottom panels*) EGFR antibodies. The cells were transduced with either vector control or AGR2 cDNA. The *scale bar* = 10 μm. *B*, 20 μg of whole cell extracts from AGR2 or vector control-transfected MCF-10A cells were resolved with a 7% SDS-PAGE gel and immunoblotted with anti-EGFR antibodies. *C*, protein immunoblots of subcellular fractions (10 μg/lane) from MCF-10A cells transfected with a vector control or AGR2 cDNA. Antibodies for EGFR, ITGB1, calnexin (*CANX*), and AGR2 were used. Calnexin serves as a marker for the microsomes. *Homo*, homogenate; *PM*, plasma membrane; *Mic*, microsomes. *D*, immune precipitates (*IP*) from *N*-ethylmaleimide (*NEM*)-treated or untreated MCF-10A cells transfected with AGR2 or vector control cDNA were collected with control IgG or mouse anti-AGR2 antibodies and detected with protein immunoblotting using rabbit anti-AGR2 antibodies. Before SDS-PAGE, the samples were unreduced (−, *left panel*) or reduced (+, *right panel*) with 0.1 M DTT. The band at ~180 kDa in the unreduced IgG lane most likely represents nonspecific binding to intact immunoglobulin. *Arrowhead*, AGR2-EGFR mixed disulfide; *arrow*, AGR2. *E*, AGR2 immune-precipitated mixed disulfides from *N*-ethylmaleimide-treated MCF-10A cells transfected with AGR2 or vector control and detected by protein immunoblotting with anti-EGFR antibodies. *Arrowhead*, EGFR. *F*, MCF-10A cells were transfected with cDNA representing AGR2, AGR2-C81A, or a plasmid vector control followed by cell surface labeling with biotin. 200 μg of cell lysates were subjected to streptavidin affinity purification. Fifteen percent of the purified proteins were assessed for EGFR and *ITGB1* with protein immunoblotting. The whole cell lysates (10 μg, *WCL*) represent 10% of the starting material used for the affinity purification and were probed with antibodies to EGFR, AGR2, and β-actin (*ACTB*). *G*, immunocytochemistry of CHO-K1 cells transiently transfected with EGFR-GFP alone (*left panel*) or EGFR-GFP + AGR2 (*right two panels*). *Green*, GFP signal from EGFR-GFP fusion protein; *red*, anti-AGR2; *blue*, DAPI. *Scale bar* = 10 μm.

TABLE 1
Viable offspring of *AGR2*$^{+/-}$ heterozygote matings

n	Males	Females	+/+	+/−	−/−
			%	%	%
52	28	24	22 (42.3)	28 (58.8)	2 (3.8)

also likely that induced *AREG* expression by EGFR is mediated by YAP1 activation as previously described (16).

The absence of another dominant AGR2 mixed disulfide (Figs. 1, *A*, *C*, and *D*, and 5*D*) suggests that EGFR is a major substrate for AGR2. None of the proteins previously reported to bind AGR2 such as LYPD3 (C4.4a), DAG1, or MUC2 (33, 46) were detected in the mass spectrometry analysis of AGR2 mixed disulfides. Re-evaluation of MUC2 in a recent study also concluded that it is not a AGR2-binding protein and that AGR2 served no role in its folding (47). The present study differed from previously identified AGR2 binding proteins by the ability to measure a biologic outcome that is shared by its substrate. In the present study similar outcomes were achieved whether *AGR2* or *EGFR* expression was reduced, thus supporting an essential functional relationship between the two proteins. Other AGR2 binding proteins are expected such as potential oxidases that will recycle AGR2 or other chaperones that may also participate in EGFR folding. We conclude, however, that AGR2's major biological effect is mediated through EGFR signaling because of the overlap in cellular effects.

EGFR's dependence on AGR2 is also supported by the newly generated knock-out mice. The approach used to generate *AGR2* null mice in the present study ensured that *AGR2* expression was disrupted, which resulted in a high rate of embryonic lethality, and closely resembled the outcome of previously generated *EGFR* null mice (41, 42). It is likely the previously published conditional null mice expressed some AGR2 at early developmental stages that increased viability (32, 33, 43). In summary, the results of the null mice support an essential role for AGR2 in EGFR-mediated signaling.

AGR2's expression pattern is also consistent with that of a regulated process. In contrast to other endoplasmic reticulum-based thioredoxins, *AGR2* is not constitutively expressed in all cells. In fact, *AGR2* is rarely expressed in most normal cells, indicating that its expression is regulated. In contrast, *AGR2* expression is present in cell lines and tissues where EGFR-mediated signaling is active. Considering the absence of AGR2 protein and transcript in most normal tissues and the widespread expression of *EGFR* transcripts, AGR2 expression represents a novel and possibly dominant post-translational mechanism for regulating EGFR-mediated cell signaling. The identification of EGFR as an AGR2 substrate provides insights into why cancer prognosis or response to therapy often does not correlate with EGFR protein or RNA levels because such measures do not reflect delivery to the cell surface (7, 48).

The number of publications reporting AGR2 expression in tumors has increased significantly and includes non-small cell lung cancer, colon cancer, breast adenocarcinoma, ovarian cancer, papillary thyroid tumors, prostate adenocarcinoma, glioblastoma, pancreatic adenocarcinoma, oral cancer, and esophageal cancers (9–15, 49–52). EGFR-mediated signaling has been reported to serve a significant role in all of these tumors. Based on this study's findings, we hypothesize that *AGR2* is expressed in all tumors with active EGFR-mediated signaling and serves as a major regulatory factor.

The present work also features AGR2 as a novel therapeutic target because it regulates EGFR at a very early stage in its life cycle. Recent studies have suggested that most, if not all, EGFR-mediated signaling occurs at the plasma membrane (5, 6), which this study demonstrates can only be achieved with AGR2 expression. Manipulation of AGR2 expression successfully disrupted EGFR-mediated signaling in cells that were resistant to a tyrosine kinase inhibitor. Other factors that may also weaken the effectiveness of current therapies include tyrosine kinase-independent EGFR functions that affect DNA synthesis, glucose uptake, and cell proliferation (53, 54). AGR2 as a therapeutic target is positioned to impact both kinase-dependent and -independent EGFR functions and represents a novel approach for inhibiting all EGFR-related activities.

Acknowledgment—We thank the Stanford Cancer Center Cores (Grant P30CA124435) for mass spectrometry, flow cytometry, and transgenic mouse services.

REFERENCES

1. Cohen, S., Fava, R. A., and Sawyer, S. T. (1982) Purification and characterization of epidermal growth factor receptor/protein kinase from normal mouse liver. *Proc. Natl. Acad. Sci. U.S.A.* **79,** 6237–6241
2. Cohen, S., Carpenter, G., and King, L., Jr. (1980) Epidermal growth factor-receptor-protein kinase interactions. Co-purification of receptor and epidermal growth factor-enhanced phosphorylation activity. *J. Biol. Chem.* **255,** 4834–4842
3. Ullrich, A., Coussens, L., Hayflick, J. S., Dull, T. J., Gray, A., Tam, A. W., Lee, J., Yarden, Y., Libermann, T. A., and Schlessinger, J. (1984) Human epidermal growth factor receptor cDNA sequence and aberrant expression of the amplified gene in A431 epidermoid carcinoma cells. *Nature* **309,** 418–425
4. Yarden, Y., Harari, I., and Schlessinger, J. (1985) Purification of an active EGF receptor kinase with monoclonal antireceptor antibodies. *J. Biol. Chem.* **260,** 315–319
5. Brankatschk, B., Wichert, S. P., Johnson, S. D., Schaad, O., Rossner, M. J., and Gruenberg, J. (2012) Regulation of the EGF transcriptional response by endocytic sorting. *Sci. Signal.* **5,** ra21
6. Sousa, L. P., Lax, I., Shen, H., Ferguson, S. M., De Camilli, P., and Schlessinger, J. (2012) Suppression of EGFR endocytosis by dynamin depletion reveals that EGFR signaling occurs primarily at the plasma membrane. *Proc. Natl. Acad. Sci. U.S.A.* **109,** 4419–4424
7. Yarden, Y., and Pines, G. (2012) The ERBB network: at last, cancer therapy meets systems biology. *Nat. Rev. Cancer* **12,** 553–563
8. Persson, S., Rosenquist, M., Knoblach, B., Khosravi-Far, R., Sommarin, M., and Michalak, M. (2005) Diversity of the protein disulfide isomerase family: identification of breast tumor induced Hag2 and Hag3 as novel members of the protein family. *Mol. Phylogenet. Evol.* **36,** 734–740
9. Hao, Y., Triadafilopoulos, G., Sahbaie, P., Young, H. S., Omary, M. B., and Lowe, A. W. (2006) Gene expression profiling reveals stromal genes expressed in common between Barrett's esophagus and adenocarcinoma. *Gastroenterology* **131,** 925–933
10. Lowe, A. W., Olsen, M., Hao, Y., Lee, S. P., Taek Lee, K., Chen, X., van de Rijn, M., and Brown, P. O. (2007) Gene expression patterns in pancreatic tumors, cells, and tissues. *PLoS ONE* **2,** e323
11. Thompson, D. A., and Weigel, R. J. (1998) hAG-2, the human homologue of the Xenopus laevis cement gland gene XAG- 2, is coexpressed with estrogen receptor in breast cancer cell lines. *Biochem. Biophys. Res. Commun.* **251,** 111–116
12. Zhang, J. S., Gong, A., Cheville, J. C., Smith, D. I., and Young, C. Y. (2005)

AGR2, an androgen-inducible secretory protein overexpressed in prostate cancer. *Genes Chromosomes Cancer* **43,** 249–259
13. Fritzsche, F. R., Dahl, E., Dankof, A., Burkhardt, M., Pahl, S., Petersen, I., Dietel, M., and Kristiansen, G. (2007) Expression of AGR2 in non small cell lung cancer. *Histol. Histopathol.* **22,** 703–708
14. Zhu, H., Lam, D. C., Han, K. C., Tin, V. P., Suen, W. S., Wang, E., Lam, W. K., Cai, W. W., Chung, L. P., and Wong, M. P. (2007) High resolution analysis of genomic aberrations by metaphase and array comparative genomic hybridization identifies candidate tumour genes in lung cancer cell lines. *Cancer Lett.* **245,** 303–314
15. Armes, J. E., Davies, C. M., Wallace, S., Taheri, T., Perrin, L. C., and Autelitano, D. J. (2013) AGR2 expression in ovarian tumours: a potential biomarker for endometrioid and mucinous differentiation. *Pathology* **45,** 49–54
16. Dong, A., Gupta, A., Pai, R. K., Tun, M., and Lowe, A. W. (2011) The human adenocarcinoma-associated gene, AGR2, induces expression of amphiregulin through hippo pathway co-activator YAP1 activation. *J. Biol. Chem.* **286,** 18301–18310
17. Wang, Z., Hao, Y., and Lowe, A. W. (2008) The adenocarcinoma-associated antigen, AGR2, promotes tumor growth, cell migration, and cellular transformation. *Cancer Res.* **68,** 492–497
18. Jessop, C. E., Watkins, R. H., Simmons, J. J., Tasab, M., and Bulleid, N. J. (2009) Protein disulphide isomerase family members show distinct substrate specificity: P5 is targeted to BiP client proteins. *J. Cell Sci.* **122,** 4287–4295
19. Rutkevich, L. A., Cohen-Doyle, M. F., Brockmeier, U., and Williams, D. B. (2010) Functional relationship between protein disulfide isomerase family members during the oxidative folding of human secretory proteins. *Mol. Biol. Cell* **21,** 3093–3105
20. Ellgaard, L., and Ruddock, L. W. (2005) The human protein disulphide isomerase family: substrate interactions and functional properties. *EMBO Rep.* **6,** 28–32
21. Gupta, A., Dong, A., and Lowe, A. W. (2012) AGR2 gene function requires a unique endoplasmic reticulum localization motif. *J. Biol. Chem.* **287,** 4773–4782
22. Feige, M. J., and Hendershot, L. M. (2011) Disulfide bonds in ER protein folding and homeostasis. *Curr. Opin. Cell Biol.* **23,** 167–175
23. Wunderlich, M., Otto, A., Maskos, K., Mücke, M., Seckler, R., and Glockshuber, R. (1995) Efficient catalysis of disulfide formation during protein folding with a single active-site cysteine. *J. Mol. Biol.* **247,** 28–33
24. Kozieł, K., Lebiedzinska, M., Szabadkai, G., Onopiuk, M., Brutkowski, W., Wierzbicka, K., Wilczyński, G., Pinton, P., Duszyński, J., Zabłocki, K., and Wieckowski, M. R. (2009) Plasma membrane associated membranes (PAM) from Jurkat cells contain STIM1 protein is PAM involved in the capacitative calcium entry? *Int. J. Biochem. Cell Biol.* **41,** 2440–2449
25. Molinari, M., and Helenius, A. (1999) Glycoproteins form mixed disulphides with oxidoreductases during folding in living cells. *Nature* **402,** 90–93
26. Cohen, S., Ushiro, H., Stoscheck, C., and Chinkers, M. (1982) A native 170,000 epidermal growth factor receptor-kinase complex from shed plasma membrane vesicles. *J. Biol. Chem.* **257,** 1523–1531
27. Llorens, F., Hummel, M., Pastor, X., Ferrer, A., Pluvinet, R., Vivancos, A., Castillo, E., Iraola, S., Mosquera, A. M., González, E., Lozano, J., Ingham, M., Dohm, J. C., Noguera, M., Kofler, R., del Río, J. A., Bayés, M., Himmelbauer, H., and Sumoy, L. (2011) Multiple platform assessment of the EGF-dependent transcriptome by microarray and deep tag sequencing analysis. *BMC Genomics* **12,** 326
28. Amit, I., Citri, A., Shay, T., Lu, Y., Katz, M., Zhang, F., Tarcic, G., Siwak, D., Lahad, J., Jacob-Hirsch, J., Amariglio, N., Vaisman, N., Segal, E., Rechavi, G., Alon, U., Mills, G. B., Domany, E., and Yarden, Y. (2007) A module of negative feedback regulators defines growth factor signaling. *Nat. Genet.* **39,** 503–512
29. Araki, K., and Nagata, K. (2011) Protein folding and quality control in the ER. *Cold Spring Harb. Perspect. Biol.* **3,** a007526
30. Kawamoto, T., Sato, J. D., Le, A., Polikoff, J., Sato, G. H., and Mendelsohn, J. (1983) Growth stimulation of A431 cells by epidermal growth factor: identification of high-affinity receptors for epidermal growth factor by an anti-receptor monoclonal antibody. *Proc. Natl. Acad. Sci. U.S.A.* **80,** 1337–1341
31. Johns, T. G., Mellman, I., Cartwright, G. A., Ritter, G., Old, L. J., Burgess, A. W., and Scott, A. M. (2005) The antitumor monoclonal antibody 806 recognizes a high-mannose form of the EGF receptor that reaches the cell surface when cells over-express the receptor. *FASEB J.* **19,** 780–782
32. Gupta, A., Wodziak, D., Tun, M., Bouley, D. M., and Lowe, A. W. (2013) Loss of anterior gradient 2 (agr2) expression results in hyperplasia and defective lineage maturation in the murine stomach. *J. Biol. Chem.* **288,** 4321–4333
33. Park, S. W., Zhen, G., Verhaeghe, C., Nakagami, Y., Nguyenvu, L. T., Barczak, A. J., Killeen, N., and Erle, D. J. (2009) The protein disulfide isomerase AGR2 is essential for production of intestinal mucus. *Proc. Natl. Acad. Sci. U.S.A.* **106,** 6950–6955
34. Chen, Y. C., Lu, Y. F., Li, I. C., and Hwang, S. P. (2012) Zebrafish agr2 is required for terminal differentiation of intestinal goblet cells. *PLoS ONE* **7,** e34408
35. Fisch, T. M., Prywes, R., and Roeder, R. G. (1987) c-fos sequence necessary for basal expression and induction by epidermal growth factor, 12-*O*-tetradecanoyl phorbol-13-acetate and the calcium ionophore. *Mol. Cell Biol.* **7,** 3490–3502
36. Lyall, R. M., Zilberstein, A., Gazit, A., Gilon, C., Levitzki, A., and Schlessinger, J. (1989) Tyrphostins inhibit epidermal growth factor (EGF)-receptor tyrosine kinase activity in living cells and EGF-stimulated cell proliferation. *J. Biol. Chem.* **264,** 14503–14509
37. Haruki, N., Kawaguchi, K. S., Eichenberger, S., Massion, P. P., Olson, S., Gonzalez, A., Carbone, D. P., and Dang, T. P. (2005) Dominant-negative Notch3 receptor inhibits mitogen-activated protein kinase pathway and the growth of human lung cancers. *Cancer Res.* **65,** 3555–3561
38. Soule, H. D., Maloney, T. M., Wolman, S. R., Peterson, W. D., Jr., Brenz, R., McGrath, C. M., Russo, J., Pauley, R. J., Jones, R. F., and Brooks, S. C. (1990) Isolation and characterization of a spontaneously immortalized human breast epithelial cell line, MCF-10. *Cancer Res.* **50,** 6075–6086
39. Puck, T. T., Cieciura, S. J., and Robinson, A. (1958) Genetics of somatic mammalian cells. III. Long-term cultivation of euploid cells from human and animal subjects. *J. Exp. Med.* **108,** 945–956
40. Slieker, L. J., and Lane, M. D. (1985) Post-translational processing of the epidermal growth factor receptor. Glycosylation-dependent acquisition of ligand-binding capacity. *J. Biol. Chem.* **260,** 687–690
41. Threadgill, D. W., Dlugosz, A. A., Hansen, L. A., Tennenbaum, T., Lichti, U., Yee, D., LaMantia, C., Mourton, T., Herrup, K., and Harris, R. C. (1995) Targeted disruption of mouse EGF receptor: effect of genetic background on mutant phenotype. *Science* **269,** 230–234
42. Sibilia, M., and Wagner, E. F. (1995) Strain-dependent epithelial defects in mice lacking the EGF receptor. *Science* **269,** 234–238
43. Zhao, F., Edwards, R., Dizon, D., Afrasiabi, K., Mastroianni, J. R., Geyfman, M., Ouellette, A. J., Andersen, B., and Lipkin, S. M. (2010) Disruption of Paneth and goblet cell homeostasis and increased endoplasmic reticulum stress in Agr2−/− mice. *Dev. Biol.* **338,** 270–279
44. Anelli, T., and Sitia, R. (2008) Protein quality control in the early secretory pathway. *EMBO J.* **27,** 315–327
45. Reddy, B. V., and Irvine, K. D. (2013) Regulation of Hippo Signaling by EGFR-MAPK signaling through ajuba family proteins. *Dev. Cell* **24,** 459–471
46. Fletcher, G. C., Patel, S., Tyson, K., Adam, P. J., Schenker, M., Loader, J. A., Daviet, L., Legrain, P., Parekh, R., Harris, A. L., and Terrett, J. A. (2003) hAG-2 and hAG-3, human homologues of genes involved in differentiation, are associated with oestrogen receptor-positive breast tumours and interact with metastasis gene C4.4a and dystroglycan. *Br. J. Cancer* **88,** 579–585
47. Bergström, J. H., Berg, K. A., Rodríguez-Piñeiro, A. M., Stecher, B., Johansson, M. E., and Hansson, G. C. (2014) AGR2, an endoplasmic reticulum protein, is secreted into the gastrointestinal mucus. *PLoS ONE* **9,** e104186
48. Arteaga, C. L. (2002) Epidermal growth factor receptor dependence in human tumors: more than just expression? *Oncologist* **7,** 31–39
49. Chen, Y. T., Ho, C. L., Chen, P. K., Chen, Y. L., and Chang, C. F. (2013) Anterior gradient 2: a novel sensitive tumor marker for metastatic oral cancer. *Cancer Lett.* **339,** 270–278
50. Li, Y., Lu, J., Peng, Z., Tan, G., Liu, N., Huang, D., Zhang, Z., Duan, C.,

Tang, X., and Tang, F. (2014) *N,N′*-dinitrosopiperazine-mediated AGR2 is involved in metastasis of nasopharyngeal carcinoma. *PLoS ONE* **9,** e92081

51. Di Maro, G., Salerno, P., Unger, K., Orlandella, F. M., Monaco, M., Chiappetta, G., Thomas, G., Oczko-Wojciechowska, M., Masullo, M., Jarzab, B., Santoro, M., and Salvatore, G. (2014) Anterior gradient protein 2 promotes survival, migration and invasion of papillary thyroid carcinoma cells. *Mol. Cancer* **13,** 160
52. Hong, X. Y., Wang, J., and Li, Z. (2013) AGR2 expression is regulated by HIF-1 and contributes to growth and angiogenesis of glioblastoma. *Cell Biochem. Biophys.* **67,** 1487–1495
53. Rauch, J., Volinsky, N., Romano, D., and Kolch, W. (2011) The secret life of kinases: functions beyond catalysis. *Cell Commun. Signal* **9,** 23
54. Weihua, Z., Tsan, R., Huang, W. C., Wu, Q., Chiu, C. H., Fidler, I. J., and Hung, M. C. (2008) Survival of cancer cells is maintained by EGFR independent of its kinase activity. *Cancer Cell* **13,** 385–393